N-methylation of a bactericidal compound as a resistance mechanism in *Mycobacterium tuberculosis*

Thulasi Warrier[a], Kanishk Kapilashrami[b], Argyrides Argyrou[c], Thomas R. Ioerger[d], David Little[a], Kenan C. Murphy[e], Madhumitha Nandakumar[a], Suna Park[a], Ben Gold[a], Jianjie Mi[a], Tuo Zhang[a], Eugenia Meiler[f], Mike Rees[c], Selin Somersan-Karakaya[g], Esther Porras-De Francisco[f], Maria Martinez-Hoyos[f], Kristin Burns-Huang[a], Julia Roberts[a], Yan Ling[a], Kyu Y. Rhee[a,g], Alfonso Mendoza-Losana[f], Minkui Luo[b,h], and Carl F. Nathan[a,1]

[a]Department of Microbiology and Immunology, Weill Cornell Medicine, New York, NY 10021; [b]Chemical Biology Program, Memorial Sloan Kettering Cancer Center, New York, NY 10065; [c]Platform Technology and Science, GlaxoSmithKline, Stevenage SG1 2NY, United Kingdom; [d]Department of Computer Science and Engineering, Texas A&M University, College Station, TX 77843-3474; [e]Department of Microbiology and Physiological Systems, University of Massachusetts Medical School, Worcester, MA 01655; [f]Diseases of the Developing World, GlaxoSmithKline (GSK), 28760 Madrid, Spain; [g]Department of Medicine, Weill Cornell Medicine, New York, NY 10021; and [h]Department of Pharmacology, Weill Cornell Medicine, New York, NY 10021

Contributed by Carl F. Nathan, June 8, 2016 (sent for review April 26, 2016; reviewed by Thomas Dick, Babak Javid, and Richard E. Lee)

The rising incidence of antimicrobial resistance (AMR) makes it imperative to understand the underlying mechanisms. *Mycobacterium tuberculosis* (Mtb) is the single leading cause of death from a bacterial pathogen and estimated to be the leading cause of death from AMR. A pyrido-benzimidazole, 14, was reported to have potent bactericidal activity against Mtb. Here, we isolated multiple Mtb clones resistant to 14. Each had mutations in the putative DNA-binding and dimerization domains of *rv2887*, a gene encoding a transcriptional repressor of the MarR family. The mutations in Rv2887 led to markedly increased expression of *rv0560c*. We characterized Rv0560c as an *S*-adenosyl-*L*-methionine-dependent methyltransferase that *N*-methylates 14, abolishing its mycobactericidal activity. An Mtb strain lacking *rv0560c* became resistant to 14 by mutating decaprenylphosphoryl-β-D-ribose 2-oxidase (DprE1), an essential enzyme in arabinogalactan synthesis; 14 proved to be a nanomolar inhibitor of DprE1, and methylation of 14 by Rv0560c abrogated this activity. Thus, 14 joins a growing list of DprE1 inhibitors that are potently mycobactericidal. Bacterial methylation of an antibacterial agent, 14, catalyzed by Rv0560c of Mtb, is a previously unreported mechanism of AMR.

antimicrobial resistance | transcription factor | methyltransferase | arabinogalactan synthesis

The World Health Organization recently announced success in meeting the millennium development goal of reversing the rise in worldwide incidence of tuberculosis (TB) by 2015 (1). Nonetheless, TB mortality remains high, with 1.5 million deaths in 2013 alone, of which 0.2 million were estimated to be caused by multidrug-resistant (MDR) strains of *Mycobacterium tuberculosis* (Mtb). MDR TB is defined as TB caused by Mtb resistant to isoniazid and rifampin, two of the four frontline TB drugs. MDR TB requires over 20 mo of treatment with toxic second-line drugs (2). Extensively drug-resistant (XDR) TB, which involves additional resistance to second-line drugs, has been detected worldwide. A recent study with a 5-y follow-up of patients with XDR TB in South Africa found that only 5% were cured, 73% died, and 10% who failed treatment but survived were discharged to the community with Mtb-positive sputum, that is, with contagious XDR TB (3). There is an urgent need to deepen our understanding of mechanisms of antimicrobial resistance (AMR). Elucidation of AMR mechanisms will help in the development of new anti-TB drugs. For example, a structural modification to a drug candidate could avoid resistance, or combination therapy could include an inhibitor of an enzyme that inactivates the drug, as when β-lactamase inhibitors are coadministered with β-lactams.

AMR in Mtb and other bacterial pathogens is heritable or phenotypic (4). Heritable AMR was observed in Mtb soon after the use of the first TB drug, streptomycin, and led to the introduction of combination chemotherapy to the practice of medicine (5). Unlike many other bacterial pathogens, mycobacteria do not readily exchange genetic material to spread resistance-causing genes; instead, accumulation of spontaneous mutations allows selection for drug resistance. Clinically, resistance to most frontline TB drugs is caused by mutations in the activation pathways of prodrugs (e.g., *katG* mutations can confer resistance to isoniazid) and/or mutations in the target (e.g., *rpoB* mutations can confer resistance to rifampicin) (6). Additional mechanisms of AMR have been described in Mtb and the fast-growing *Mycobacterium smegmatis* (7). Some are nonspecific, such as increased expression of the efflux pumps Tap and IniBAC (8, 9). Others involve direct modification and inactivation of the drug, such as expression of the β-lactamase BlaC that hydrolyzes β-lactams (10) and the acetyl transferase Eis that acetylates and inactivates kanamycin (11). Target modification plays a role in macrolide resistance through methylation of 23S rRNA by the Erm family of methyl transferases (12). However, to the best of our knowledge, inactivation of an antibiotic by its methylation has not been reported.

The goal of this study was to determine the mechanism of resistance to and mode of action of 14 (Fig. 1*A*), which was recently

Significance

Better understanding of the mechanisms used by bacteria to counter antibacterial agents is essential to cope with the rising prevalence of antimicrobial resistance. Here, we identified the mechanism of resistance of *Mycobacterium tuberculosis* to an antimycobacterial cyano-substituted fused pyrido-benzimidazole. Clones bearing mutations in a transcription factor, Rv2887, markedly up-regulated the expression of *rv0560c*, a putative methyltransferase. Rv0560c *N*-methylated the pyrido-benzimidazole in vitro and in *Mycobacterium tuberculosis*, abrogating its bactericidal activity. Resistant mutants selected in the absence of *rv0560c* led to the identification of the target of the compound, the essential oxidoreductase, decaprenylphosphoryl-β-D-ribose 2-oxidase (DprE1). Methylation of an antibacterial compound is a previously uncharacterized mode of antimicrobial resistance.

Author contributions: T.W., K.K., A.A., M.L., and C.F.N. designed research; T.W., K.K., A.A., T.R.I., D.L., K.C.M., M.N., S.P., J.M., E.M., M.R., S.S.-K., E.P.-D.F., M.M.-H., J.R., and Y.L. performed research; K.C.M. and A.M.-L. contributed new reagents/analytic tools; T.W., K.K., A.A., T.R.I., K.C.M., M.N., S.P., B.G., J.M., T.Z., E.M., K.B.-H., K.Y.R., A.M.-L., M.L., and C.F.N. analyzed data; and T.W. and C.F.N. wrote the paper.

Reviewers: T.D., National University of Singapore Yong Loo Lin School of Medicine; B.J., Tsinghua University School of Medicine; and R.E.L., St. Jude Children's Research Hospital.

The authors declare no conflict of interest.

Freely available online through the PNAS open access option.

Data deposition: The RNASeq data described in *SI Appendix*, Table S1 have been deposited in the Gene Expression Omnibus (GEO) database, www.ncbi.nlm.nih.gov/geo (accession no. GSE77556).

[1]To whom correspondence should be addressed. Email: cnathan@med.cornell.edu.

This article contains supporting information online at www.pnas.org/lookup/suppl/doi:10.1073/pnas.1606590113/-/DCSupplemental.

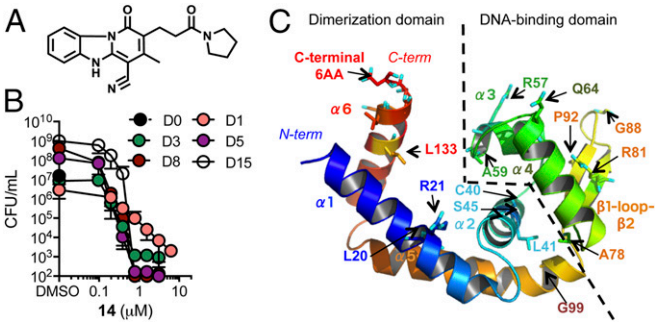

Fig. 1. Activity of 14 and the Rv2887 mutations identified in 14-resistant Mtb clones. (*A*) Structure of 14. (*B*) Kinetics of bactericidal activity of 14 against Mtb as measured by cfu counts on postexposure days 1, 3, 5, 8, and 15. (*C*) Phyre 2 generated homology model of Rv2887 highlighting the 16 unique mutations identified in Mtb clones resistant to 14. The secondary structure elements are color coded as described: blue, α1 helix; light blue, α2 helix; light green, α3 helix; dark green, α4 helix; orange, β1–loop–β2 region; dark red, α5 helix; and red, α6 helix. The dashed line demarcates the predicted dimerization and DNA-binding domains.

identified as bactericidal to replicating Mtb (13). We identified the mechanism of resistance as *N*-methylation of compound 14 by a previously uncharacterized methyltransferase, Rv0560c. After the resistance mechanism was incapacitated by genetic deletion of *rv0560c*, selection of additional mutants at a far lower frequency allowed us to identify the target of 14 as decaprenylphosphoryl-β-D-ribose 2-oxidase (DprE1), an essential enzyme involved in arabinogalactan synthesis.

Results

Sterilizing Activity of 14 in Vitro. Earlier work showed that 14 inhibits Mtb growth with an IC_{90} of 0.39 μM and that the compound is bactericidal under conditions that support bacterial replication (13). In the present studies, we found that 14's mycobactericidal activity was dose- and time-dependent, with a multilog reduction in colony-forming units observed at 0.78 μM after a brief exposure of 3 d and further colony-forming unit reduction to below the limit of detection by 8 d (Fig. 1*B*). A recent study reported that some antimycobacterial compounds with potent activity in vitro were inactive in vivo because glycerol was used as the carbon source in the in vitro experiments (14). However, we observed no change in the IC_{90} of 14 when glycerol, dextrose, or acetate served as the carbon source (*SI Appendix*, Fig. S1).

Resistance to 14 Is Associated with Mutations in *rv2887*. To elucidate the mode of action of 14, we isolated resistant clones after incubation of Mtb at 4-, 5-, 10-, or 20-fold the IC_{90} of 14 and observed a frequency of resistance of 1–3 × 10^{-7} (*SI Appendix*, Fig. S2*A*). Whole genome resequencing of four resistant clones (highlighted in Table 1) found one gene, *rv2887*, to be mutated in common. Rv2887 is annotated as a nonessential, putative transcription factor. Amino acid sequence analysis predicted that Rv2887 has the winged helix–turn–helix DNA binding domain found in the MarR family of transcription factors (*SI Appendix*). Mtb has at least six other genes that belong to this family, namely, *rv0042c*, *rv0737*, *rv0880*, *rv1049*, *rv1404*, and *rv2327*. These proteins share homology with MarR, the transcriptional repressor of *Escherichia coli* linked to the multiple antibiotic resistance (mar) phenotype. Resequencing of *rv2887* in 16 additional resistant clones revealed 12 additional SNPs leading to missense or nonsense mutations (Table 1).

We used Phyre 2 (15) to build a homology model of Rv2887 that predicted an α1–α2–α3–α4–β1–loop–β2–α5–α6 topology, as observed in crystal structures of *E. coli* MarR and its homologs (Fig. 1*C*) (16). The N-terminal α1–α2 helices and C-terminal α5–α6 helices of a MarR monomer interact with the corresponding regions

Table 1. Characterization of Mtb clones resistant to 14

Strain name*	IC_{90} of 14, μM	SNP in *rv2887*	Mutation in Rv2887	Other SNPs	Fold change in IC_{90} of RIF
WT	0.39	—	—	—	—
1A	12.5	G242A	R81Q	Rv0516c:L69M, plcB:R190R, 3418802 A > G	1
2A	12.5	C274T	P92S	None in DprE1	0.5
5A	12.5	T122C	L41P	Rv0516c:L69M, plcB:R190R, 3418802 A > G	1
6A	25	G62A	R21Q	Rv1619:Y457H, Rv2173/idsA2:S201P	1
8A	>25	G400T	C-term 6 AA deletion and addition of 61 AA	Rv0560c:S140A	1
10A	25	G296T	G99V	None in DprE1	0.25
12A	12.5	C274T	P92S	None in DprE1	0.5
15A	12.5	G242A	R81Q	None in DprE1	0.5
17A	12.5	A191C	Q64P	—	1
183A	12.5	Insertion of 14 nts after G125 leading to stop codon after AA45	Stop codon after 45AA	None in DprE1	1
183B	25	G263A	G88E	None in DprE1	1
183C	12.5	T59C	L20P	None in DprE1	1
189A	12.5	C176A	A59E	None in DprE1	1
195A	6.25	G119T	C40F	None in DprE1	1
195B	6.25	G170A	R57Q	None in DprE1	1
195C	6.25	G119T	C40F	None in DprE1	1
195D	6.25	T398C	L133P	None in DprE1	1
195E	6.25	G232C	A78P	None in DprE1	1
195F	6.25	C136T	Stop codon after 45AA	None in DprE1	1
195H	6.25	T398C	L133P	None in DprE1	1

*The names of strains analyzed by whole genome resequencing are in bold. RIF, rifampin.

in a second monomer to form the functional dimer (16). Previous studies with *E. coli* mutant strains showed that point mutations or deletions in the N or C termini of MarR led to loss of repressor activity (17, 18). Nine of the 16 unique mutations in our resistant clones mapped to the homologous regions of Rv2887 (Fig. 1*C* and Table 1). The winged helix fold in MarR, formed by the third and fourth helices and the β–loop–β sheet domain, is predicted to bind the promoter region of the *marRAB* operon in *E. coli*, and the remaining seven unique mutations in our resistant clones mapped to the homologous domain of Rv2887 (Fig. 1*C* and Table 1). Three of the mutated residues identified in Rv2887—R81, G99, and Q64—are homologous to MarR residues reported to be essential for DNA binding in *E. coli*, where they correspond to R86, G104, and G69, respectively (17, 19). R86 and G104 are among the most highly conserved residues among MarR homologs across different species (16, 17, 19). Thus, each of the Rv2887 mutations identified in the resistant clones is likely to cause complete or partial loss of the DNA binding function of Rv2887.

Specific Role of Rv2887 in Mediating Resistance to 14. *E. coli* mutants lacking MarR and MarA are resistant to diverse antibiotics and other stresses (20, 21). To determine if Rv2887 fulfilled a similar role in Mtb, we tested susceptibility of two resistant clones, 1A and 8A, to the TB drugs rifampin, isoniazid, ethambutol, moxifloxacin, and streptomycin and did not observe increased resistance or susceptibility relative to wild-type strain (*SI Appendix*, Fig. S2*B*). Replacement of the wild-type allele of *rv2887* in Mtb with mutant allele carrying the point mutations found in these two resistant clones, namely R81Q (as found in clone 1A) or deletion of six amino acids at the C terminus (as found in clone 8A), by oligonucleotide-mediated recombineering (22), conferred resistance specifically to 14 (Fig. 2*A* and *SI Appendix*, Fig. S2*C*). However, introduction of the *rv2887* mutation found in resistant clone 8A into wild-type Mtb did not lead to a level of resistance as high as that displayed by clone 8A itself (IC_{90} > 25 μM). This data suggested that additional mutations in clone 8A might contribute to its high level of resistance. Whole genome resequencing of clone 8A revealed an additional SNP leading to S140A mutation in Rv0560c, whose significance emerged in studies described below. To confirm the role of Rv2887 in resistance to 14, wild-type *rv2887* was overexpressed in the resistant clones 1A and 8A. Overexpression of *rv2887* increased the susceptibility of both clones to 14 (Fig. 2*A*).

Genes and Pathways Regulated by Rv2887. Based on similarity of Rv2887 to the transcriptional repressor MarR, we hypothesized that loss-of-function mutations in Rv2887 lead to derepression of the target of 14 or of genes linked to the target pathway. RNAseq gene expression profiles of the wild-type strain and the resistant clones 1A and 8A were generated after 4 h of exposure to 14 or vehicle (DMSO). In the absence of compound treatment, resistant clones 1A and 8A had a common set of 13 up-regulated genes and 17 down-regulated genes, relative to the wild-type strain (*SI Appendix*, Table S1). The gene with the largest increase in expression—~400-fold—was *rv0560c*, annotated as a putative, nonessential benzoquinone methyltransferase. The gene *rv0559c*, which is predicted to be in the same operon as *rv0560c*, was up-regulated by ~15-fold in vehicle-treated resistant clones. Two genes transcribed in the opposite direction from the *rv0560c* operon, *rv0557* and *rv0558*, were also up-regulated in the resistant clones, by ~threefold and ~20-fold, respectively. Unlike *E. coli marR*, which is self-regulated, *rv2887* expression was not altered in the resistant clones. The down-regulated genes included the tRNA and noncoding RNA transcripts *asnT*, *argV*, and *mpr11* (*SI Appendix*, Table S1), but no protein-coding transcripts.

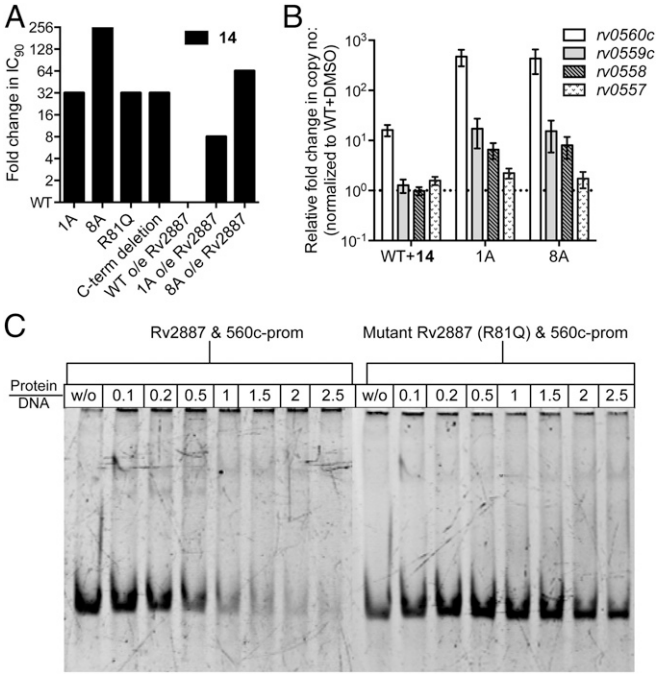

Fig. 2. Role of *rv2887* in resistance to 14 and genes regulated by Rv2887 in Mtb. (*A*) Fold changes in IC_{90} of 14 relative to wild-type Mtb H37Rv (WT) are shown. The strains tested are two clones resistant to 14, 1A and 8A; wild-type strains carrying the two Rv2887 mutations, R81Q and C-terminal deletion, found in clones 1A and 8A; and three strains, WT, 1A, and 8A, that express *rv2887* constitutively (WT o/e *rv2887*, 1A o/e *rv2887*, and 8A o/e *rv2887*). o/e, overexpression. (*B*) Relative change in expression of *rv0560c*, *rv0559c*, *rv0558*, and *rv0557* in wild-type Mtb H37Rv (WT) treated with 3.9 μM of 14 for 4 h and two resistant clones, 1A and 8A, that were vehicle-treated for 4 h. The baseline of 1 indicates expression level in Mtb H37Rv treated with vehicle control. (*C*) Native PAGE gels of wild-type Rv2887 or mutant Rv2887, with the point mutation R81Q, incubated with a 70-bp DNA sequence spanning the promoter of *rv0560c* (560c-prom).

The RNAseq results thus directed our attention to the cluster of four protein-coding genes up-regulated in the *rv2887* mutants, *rv0557–rv0560c*. Quantitative reverse transcriptase (qRT) PCR (Fig. 2*B*) confirmed that *rv0560c*, *rv0559c*, and *rv0558* were significantly up-regulated (>fivefold) in the resistant clones, whereas *rv0557* was not. Finally, *rv0560c* was found to be up-regulated by ~eightfold and ~40-fold as detected by qRT-PCR (Fig. 2*B*) and RNA Seq (*SI Appendix*, Table S1), respectively, in wild-type Mtb exposed to 3.9 μM (~10× IC_{90}) of 14 for 4 h. In contrast, exposure of wild-type Mtb to 14 did not affect expression of *rv0559c* and *rv0558*. Based on these data, we predicted a model in which Rv2887 acts as a repressor of *rv0560c* and loss-of-function mutations in Rv2887 lead to derepression and thus increased expression of *rv0560c*.

Rv2887 Binds to the Promoter Region of *rv0560c*. Previous characterization of the promoter region of *rv0560c* identified the putative −35 and −10 elements and predicted a putative repressor binding site (23). We determined if recombinant Rv2887 (*SI Appendix*, Fig. S3*A*) could bind the 70-bp region spanning the reported promoter region of *rv0560c* (560c-prom) (*SI Appendix*, Table S2). Migration of the oligonucleotide in the gel was retarded by ≥1 molar equivalent of Rv2887 (Fig. 2*C*). Quantitative analysis of band intensities indicated 50% reduction in the unbound DNA at 1.5 molar equivalent of Rv2887 (*SI Appendix*, Fig. S4). Rv2887 did not bind to a 36-bp region corresponding to the promoter region of an IdeR-regulated gene, *mbtB* (mbtB-prom) (*SI Appendix*, Fig. S4) (24). Our observation that Rv2887 regulates

expression of Rv0560c is supported by a recent genome-wide analysis of regulatory interactions in Mtb using ChIP-Seq- and RNA-Seq-based assays (25). Introduction of the R81Q mutation into Rv2887 abolished its ability to bind 560c-prom DNA (Fig. 2*C* and *SI Appendix*, Fig. S4), providing direct evidence that the mutation present in resistant clone 1A impacts ability of Rv2887 to bind the promoter region of *rv0560c*. We also examined the impact of mutations in 560c-prom DNA sequence, both those in palindromic regions and those previously reported to affect repression (23), on binding by Rv2887 in vitro, and observed a mild effect at ≥2 molar equivalents of Rv2887 (*SI Appendix*, Fig. S4).

Rv0560c Methylates and Inactivates 14. We hypothesized that upregulation of *rv0560c*, *rv0558*, or *rv0559c* could be contributing to the resistance phenotype of the clones, 1A and 8A. We tested susceptibility of wild-type Mtb individually overexpressing each of these genes to 14. Mtb became 16-fold more resistant to 14 when *rv0560c* was overexpressed, whereas overexpression of *rv0558* and *rv0559c* had no impact on sensitivity to 14 (Fig. 3*A* and *SI Appendix*, Fig. S5). Because Rv0560c is reportedly nonessential (26), we reasoned that it was unlikely to be the target of 14. Instead, given that increased expression of Rv0560c conferred resistance to 14 on the wild-type strain, we hypothesized that Rv0560c inactivates 14, directly or indirectly. Moreover, given that the most resistant mutant was clone 8A, which carried mutations in both *rv2887* and *rv0560c*, we predicted that the S140A mutation in Rv0560c might augment the ability of Rv0560c to inactivate 14.

Based on the putative methyltransferase activity of Rv0560c, we tested recombinant Rv0560c and S140A-Rv0560c (*SI Appendix*, Fig. S3*B*) for methyltransferase activity with 14 as the candidate substrate. After overnight coincubation of 14 with *S*-adenosyl-*L*-methionine (SAM) and Rv0560c, mass spectrometry coupled to liquid chromatography (LC-MS) analysis detected an additional peak with an *m*/*z* of 363.18, which is 14 mass units (CH_2 group) greater than that of 14 (*SI Appendix*, Fig. S6). We then examined the kinetics of methylation of 14 by Rv0560c and S140A-Rv0560c by taking advantage of the characteristic blue shift at 380 nm observed in the absorption spectrum of 14 upon methylation (*SI Appendix*, Fig. S7*A*). Initial velocity of the methylation reaction, as reflected by the absorbance changes at 380 nm, depended on the concentration of Rv0560c (*SI Appendix*, Fig. S7*B*). Although wild-type Rv0560c can modify 14, the substrate turnover measured by k_{cat} was increased by 2.4-fold for S140A-Rv0560c (Fig. 3*B*). Enhancement was even greater when *S*-adenosyl-*L*-homocysteine (SAH) was depleted by two coupled enzymes, 5′-methylthioadenosine/*S*-adenosylhomocysteine nucleosidase (MTAN) and adenine deaminase (*SI Appendix*, Fig. S7*C*). SAH, the common byproduct of methylation, is often characterized as a pan-inhibitor of methyltransferases and can be rapidly degraded inside cells by other metabolic enzymes, as mimicked by the addition of the coupling enzymes mentioned above (27). Given that S140 is predicted to be near to a putative SAM binding site, the increased methyltransferase activity of S140A-Rv0560c relative to wild-type Rv0560c may be attributed to increased k_{cat}/K_m, decreased SAH inhibition, or a combination of both.

We then sought to determine the site of methylation on 14 using NMR. Comparison of ^{1}H-NMR spectra of 14 and its methylation product, me-14, revealed the nascent methyl group at 4.1 ppm (Fig. 3*C*). The ^{1}H–^{1}H COSY [number of scans (ns) = 8] allowed us to assign all of the peaks in ^{1}H spectra of 14. A gradient NOESY experiment was set up with the optimal mixing time of 0.8 s for the characteristic methyl group of me-14 (ns = 32). An NOE cross-peak between 4.1 ppm and the doublet around 7.3 ppm (C-6 proton) indicated that N-5 is the site of methylation (Fig. 3*C*). Similar assays were conducted with an analog of 14, 14-IA (*SI Appendix*, Fig. S8), which has a methyl group at N-5 and was inactive against Mtb (Fig. 3*D*). As expected, a characteristic NOE cross-peak was observed between the C-6 doublet of the analog 14-IA at 7.3 ppm and the N-5 methyl proton at 4.1 ppm (*SI Appendix*, Fig. S8). We conclude that Rv0560c is an *N*-methyltransferase that modifies 14 at the N-5 position.

We used Rv0560c to generate me-14 in vitro, extracted it from the reaction mixture, and tested it against wild-type Mtb. Like the synthetically prepared analog 14-IA, me-14 did not inhibit growth of Mtb (Fig. 3*D*), confirming that resistance to 14 can arise by its inactivation upon *N*-methylation by Rv0560c.

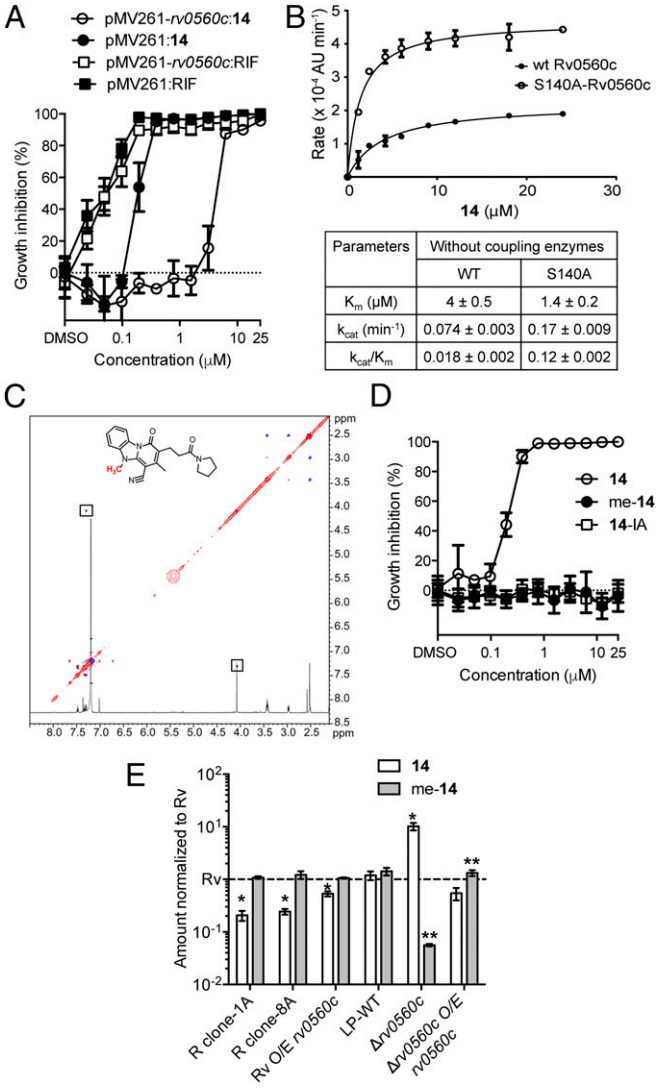

Fig. 3. Role of Rv0560c in resistance of Mtb toward 14. (*A*) IC_{90} curve of 14 and rifampin (RIF) against wild-type Mtb strain that constitutively expresses *rv0560c* (pMV261-*rv0560c*) or the vector control strain (pMV261). (*B*) Michaelis–Menten kinetics of the SAM-dependent methylation of 14 by wild-type Rv0560c (WT) protein and S140A-Rv0560c protein in the absence of coupling enzymes. Table lists the steady-state kinetic parameters of the reactions. (*C*) Overlay of the 1D ^{1}H spectrum and the NOESY spectra of me-14 with a schematic highlighting the site of methylation. (*D*) Activity of purified methylated 14 (me-14), 14, and the inactive analog, 14-IA, which is methylated at the N-5 position. (*E*) Normalized (relative to wild-type Mtb H37Rv, Rv) quantification of 14 and me-14 in the two 14-resistant clones, 1A and 8A, in the wild-type strain that constitutively expresses *rv0560c* (Rv O/E *rv0560c*), in Δ*rv0560c*, its wild-type background strain, H37Rv London Pride (LP), and Δ*rv0560c* complemented with a constitutive expression vector for *rv0560c* (Δ*rv0560c* O/E *rv0560c*). All strains were treated with 7.8 μM 14 for 24 h. (**P* < 0.05; ***P* value < 0.01, with two-tailed unpaired *t* test analysis.)

Methylation Reduces the Level of 14 in Resistant Clones. We next sought to relate the foregoing in vitro observations to the mechanism of resistance within mutant Mtb. To do this, we treated bacteria with 7.8 μM (~20× IC_{90}) of 14 for 24 h and measured intrabacterial levels of 14 and me-14 in resistant clones and in wild-type Mtb overexpressing *rv0560c*. There was no significant increase in the amount of me-14 in the resistant clones relative to the wild-type strain (H37Rv North strain, Rv), either inside the bacteria or in the extracellular medium (Fig. 3*E* and *SI Appendix*, Fig. S9). However, the amount of parent compound, 14, was reduced by fivefold in the resistant clones and by twofold in the *rv0560c*-overexpressing strain (Fig. 3*E*). The unchanged levels of me-14 in these cells might be due to the brief exposure to a large excess of 14. Moreover, these observations raise the possibility that me-14 may be subject to further modifications in Mtb. In contrast, levels of me-14 in a Δ*rv0560c* strain were 20-fold lower than in the wild-type control strain (H37Rv London Pride strain, LP), accompanied by a ~10-fold increase in 14 (Fig. 3*E*). Both differences were reversed by constitutive expression of *rv0560c* in the knockout strain (Fig. 3*E*). Collectively, these studies established that Rv0560c catalyzes the methylation of 14 within Mtb.

DprE1 Mutations Confer Resistance to 14 in the Absence of Rv0560c. To circumvent selection of resistant clones carrying *rv2887* or *rv0560c* mutations, we isolated resistant clones in the Δ*rv0560c* background. The observed frequency of resistance to 14 in Δ*rv0560c* strain was 100-fold lower than for wild-type Mtb and ranged between 0.5×10^{-9} and 8.5×10^{-9} (*SI Appendix*, Fig. S10*A*). Three of the four analyzed clones carried a point mutation, P116S, in *dprE1*, an essential gene involved in synthesis of decaprenylphosphoryl-β-D- arabinose (DPA) (*SI Appendix*, Fig. S10*B*). Introduction of this mutation into wild-type Mtb by replacing the wild-type allele with oligonucleotide-mediated recombineering led to a 16-fold increase in IC_{90} (Fig. 4*A*). These data indicated that DprE1 could be the main target of 14, and this possibility was tested as described in *Inhibition of DprE1 by 14*. Whole genome resequencing of four clones identified common mutations in *rv0678*, the putative regulator of the MmpL5-S5 transporter system, in all four clones (*SI Appendix*, Fig. S10*B*) (28). Hence, increased efflux of 14 through MmpL5 might occur in these resistant clones in addition to reduced inhibition of DprE1.

Inhibition of DprE1 by 14. Using a previously reported fluorescence-based assay (29) to monitor inhibition of pure, recombinant Mtb DprE1 by 14, we observed an IC_{50} of 70 nM against DprE1 (Fig. 4*B*). Preincubation of 14 with Rv0560c in the presence of SAM led to a 36-fold increase in the IC_{50} (Fig. 4*B*). Thus, 14 is a potent inhibitor of DprE1, and methylation by Rv0560c markedly reduced this activity. Based on the proximity of the P116 residue to the flavin adenine dinucleotide (FAD) cofactor-binding site in DprE1, we hypothesized that displacement of FAD by 14 might be the mechanism of its DprE1 inhibition. We monitored release of FAD in the presence of 14, but no release was detected (*SI Appendix*, Fig. S11*A*). A 20-fold increase in FAD fluorescence would have been observed if there was release (29); instead, binding of 14 to DprE1 caused a slight quench in FAD fluorescence (*SI Appendix*, Fig. S11*A*). We analyzed DprE1 by mass spectrometry after incubation with 14 and the substrate farnesylphosphoryl-β-D-ribose (FPR) to monitor the formation of covalent adducts by the inhibitor, but none were detected (*SI Appendix*, Fig. S11*B*). This data is also consistent with the inhibition assay data, which showed no evidence of time-dependent inhibition.

Recent studies have described six mutations in DprE1, namely C387S (30), Y314H (31), L368P (32), G17C (32), E221Q (29), and G248S (29), associated with resistance to inhibition of the enzyme by diverse molecular scaffolds. We interrogated the roles of these residues in the interaction of 14 with DprE1 by measuring

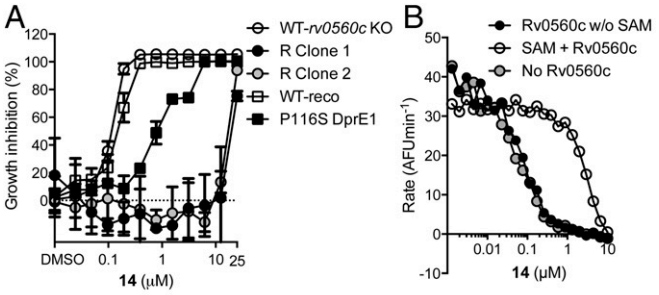

C

Fold change in IC_{90}/ Mutation in DprE1	P116S	Y314H	C387S	L368P	G17C	E221Q	G248S	O/E *dprE1*
14	16	2	1.5	8	2	32	6	>64
TCA1	16	32	8	8	2	8	4	64
BTZ-043	0.5	1	64	1	1	4	1	>64
EMB	0.5	1	1.3	1.5	1.5	0.8	1.3	1
RIF	1	1	1	0.5	1	1	1	1
INH	1.3	1.3	1.3	1.3	1.3	1.3	1.3	1

Fig. 4. Compound 14 targets Mtb DprE1. (*A*) IC_{90} curve of 14 against two resistant clones, R Clone 1 and 2, isolated in the Δ*rv0560c* background, which is referred to as WT-*rv0560c* KO. Activity against the recombineered H37Rv strain carrying only the DprE1 P116S point mutation (P116S DprE1) and its wild-type control strain (WT-reco) are also shown. (*B*) Concentration-dependent activity of 14 against DprE1 as detected by a fluorescence-based assay is depicted by grey symbols. Activity of 14 against DprE1 after pre-incubation with 10 μM Rv0560c and 300 μM SAM for 6.5 h is depicted by clear symbols, and the control without SAM is shown by black symbols. (*C*) Activity of 14, the known DprE1 inhibitors TCA1 and BTZ-043, ethambutol (EMB), rifampin (RIF), and isoniazid (INH) against Mtb H37Rv strains carrying the listed point mutations in DprE1. Mutations highlighted in red were introduced into the wild-type Mtb strain by oligonucleotide-based recombineering.

the IC_{90} of 14 against Mtb strains carrying these point mutations (Fig. 4*C*). The greatest resistance to 14 (~16- to 32-fold increase in IC_{90}) was seen in the strains in which either P116 or E221 were mutated. A milder effect (~sixfold to eightfold increase in IC_{90}) was observed when L368 or G248 were mutated. The covalent inhibitor BTZ043 was inactive only when C387, the key residue with which it forms a covalent bond with DprE1, was mutated. The activity of TCA1 was dramatically reduced when Y314 or P116 were mutated. None of these mutations affected the activity of ethambutol, isoniazid, and rifampin. Finally, overexpression of DprE1 conferred resistance to 14, as it did to the DprE1 inhibitors TCA1 and BTZ043 (Fig. 4*C*).

Discussion

We have uncovered *N*-methylation of antimicrobial compounds as a novel mechanism of AMR. Mtb exploits this mechanism to counter the antimycobacterial action of a potent pyrido-benzimidazole, 14, with bactericidal activity against replicating Mtb. The nonessential gene *rv0560c*, annotated as a putative benzoquinone methyltransferase, was found to inactivate 14 by catalyzing the transfer of a methyl group from SAM to the N-5 position. Mtb clones resistant to 14 up-regulated expression of *rv0560c* by incurring mutations in the transcriptional repressor, Rv2887. Winglee et al. (33) recently reported a role for Rv2887 in Mtb's resistance to imidazo[1,2-a] pyridine-4-carbonitrile (MP-III-71), a compound with structural similarity to 14. That study also documented up-regulation of *rv0560c* in the setting of resistance-conferring mutations in *rv2887*, but did not directly implicate Rv0560c in resistance nor establish a biochemical mechanism for mycobacterial resistance to MP-III-71.

Methylation now joins a list of covalent modifications of antibacterial compounds by which bacteria can manifest AMR,

including acetylation, phosphorylation, adenylation, and hydrolysis (34). Previous studies have shown that some proportion of intrabacterial para-amino salicylic acid (PAS) is methylated in PAS-sensitive Mtb treated with PAS (35). However, methylation of PAS by Mtb has not been observed to cause PAS resistance (36). Bacterial methyltransferases of the Erm family contribute to AMR by modifying the target of macrolides, rRNA, but those methyltransferases do not act on the macrolides themselves. Rv0560c-mediated inactivation of 14 is, to our knowledge, the first instance of compound methylation as a resistance mechanism in a bacterial species.

It is unclear how Mtb senses 14 such that a consequence is the relief of repression of *rv0560c*. One hypothesis is that 14 directly binds to Rv2887. Alternatively, an endogenous metabolite associated with DprE1 inhibition may accumulate as a consequence of its inhibition and bind to Rv2887, initiating a response to the stress of cell wall synthesis blockade. Diverse stresses, including salicylate, membrane depolarizers (carbonyl cyanide *m*-chlorophenyl hydrazone, valinomycin, or dinitrophenol), the detergent SDS, and the respiratory inhibitors chlorpromazine and thioridazine, can up-regulate *rv0560c* expression (www.tbdb.org/expressionHistory.shtml?gn=Rv0560c). We hypothesize that this occurs by the dissociation of Rv2887, the repressor, from the *rv0560c* promoter region. This theory is corroborated by the very low number of *rv0560c* transcripts in untreated, wild-type Mtb (*SI Appendix*, Table S1), compared with the marked up-regulation of *rv0560c* in Mtb strains carrying mutations in Rv2887 (Fig. 2*B*) and demonstration of a direct interaction of Rv2887 with the promoter region of *rv0560c* in a mobility shift assay (Fig. 2*C*). Although PAS, chlorpromazine, and thioridazine have been reported to up-regulate *rv0560c* gene expression, we did not observe increased resistance to these compounds in the clones 1A and 8A, which have markedly higher *rv0560c* transcripts (*SI Appendix*, Fig. S12). It is unclear how Rv0560c, a putative cytoplasmic enzyme, inactivates 14 before 14 targets DprE1, whose activity has been localized to the Mtb cell wall (37). There may be an uptake mechanism for 14 that delivers most of it from the extracellular medium to the cytosol before it can reach DprE1 in the periplasm, or perhaps marked increase in expression of Rv0560c results in some of the enzyme becoming periplasmic.

Two other MarR homologs in Mtb, Rv1049 (MosR) and Rv1404, have been shown to respond to physiologically relevant stresses. For example, exposure to hydrogen peroxide or nitric oxide led to dissociation of MosR from DNA and subsequent up-regulation of the putative oxidoreductase Rv1050 (38). Rv1404 was involved in Mtb's response to acid and hypoxia by up-regulating 10 genes, including two putative methyl transferases, Rv1403c and Rv1405c (39).

The P116S mutation in DprE1 that we found to confer resistance to 14 is different from the mutations that confer resistance to several other DprE1 inhibitors. Covalent inhibitors of DprE1 exemplified by BTZ043 select for the C387S substitution in DprE1 because they require Cys-387 to form adducts. TCA1 requires Tyr-314 for its inhibition of DprE1. Compound 14 was active against Mtb clones carrying both the C387S and Y314H mutations, indicating that its interaction with DprE1 occurs by a mechanism distinct from that of BTZ043 and TCA1. In contrast, 14 selects for the P116S mutation in DprE1. Pro-116 is adjacent to the FAD binding pocket in the DprE1 active site. Compound 14 is predicted to be largely planar, similar to the isoalloxazine ring system of the FAD. Although 14 did not displace FAD from the enzyme, it might engage in a π-stacking interaction with the FAD in the substrate-binding site, thus inhibiting enzymatic turnover by competing with the substrate.

In conclusion, our analysis of Mtb's resistance mechanism to the inhibitor, 14, revealed that a bactericidal compound could be inactivated by methylation. To the best of our knowledge, this is the first report of *N*-methylation as a strategy for bacterial drug resistance. The target of 14 is DprE1, the essential oxidoreductase involved in DPA synthesis, leading to inhibition of cell wall synthesis and death of mycobacteria. Knowledge of the resistance mechanism provides a mechanistic rationale to overcome resistance to this class of antimycobacterial agents. We established that the mycobacterial enzyme catalyzing this reaction, Rv0560c, can serve as an *N*-methyl transferase. It remains for further study to identify the physiologic roles of Rv2887 and Rv0560c in Mtb not exposed to xenobiotics.

Methods

Materials. Mtb strains were grown in Difco Middlebrook 7H9 (BD Biosciences) medium with 0.2% glycerol, 10% (vol/vol) OADC (BD Biosciences) or ADN (0.5% BSA; Roche, 0.2% dextrose, 0.085% NaCl) and 0.02% tyloxapol, or plated on 7H11 agar (BD Biosciences) supplemented with 10% (vol/vol) OADC (BD Biosciences) and 0.5% glycerol; 7H10 agar (BD Biosciences) supplemented with 10% (vol/vol) ADN and 0.5% glycerol was used to grow Mtb strains on PVDF filters (Durapore) to quantify intrabacterial abundance of 14. Mtb H37Rv North strain (Rv) was used as the wild-type strain, unless otherwise specified. The strain deficient in *rv0560c* (Δ*rv0560c*) and its wild-type background strain, H37Rv London Pride (LP), were a kind gift from Tanya Parish, Infectious Disease Research Institute, Seattle, and the strains carrying the point mutations C387S (30), L368P, and G17C (32) in DprE1 were a kind gift from Stewart Cole, École Polytechnique Fédérale de Lausanne, Lausanne, Switzerland. Compound 14 was provided by GSK or purchased from Vitas Lab (Cat#STK717481). Compound 14-IA was provided by GSK. Rifampin, isoniazid, TCA1 (Life Chemicals), and BTZ-043 (Selleckchem) were obtained from commercial vendors. MTAN was purified as described (40), and adenine deaminase was purchased from G-Biosciences. All other reagents were purchased from Sigma-Aldrich unless otherwise specified.

IC_{90} and Colony-Forming Unit Assays. Mtb strains were grown to log phase and diluted to an optical density (OD_{580}) of 0.005 in 7H9 medium. Then 200 μL/well of the Mtb suspension was dispensed in 96-well plates (Costar), and compounds were added. OD_{580} was read after 10–14 d of incubation at 37 °C with 20% O_2, 5% CO_2. IC_{90} was defined as the concentration that led to ≥90% growth inhibition. The Resazurin Microtiter Assay was used to measure IC_{90} of compounds against strains carrying the Y314H, E221Q, G248S, C387S, L368P, and G17C mutations in DprE1, as described (41). Colony-forming unit assays were set up after exposure of a single-cell suspension of Mtb in 7H9 medium at an OD_{580} of 0.005 to various concentrations of 14. At each time point, the samples were mixed, diluted 10-fold in PBS with tyloxapol (0.02%), and spread on 7H11 agar plates. Plates were incubated at 37 °C for 21–25 d, and colonies were counted.

Generation of Constructs for Constitutive Expression of Genes in Mtb and for Expression and Purification Proteins from *E. coli*. Details of the cloning strategy and the primers used for cloning are included in *SI Appendix*.

Isolation of Mtb Clones Resistant to 14 and Whole Genome Sequencing. Log phase culture of Mtb H37Rv, LP, or Δ*rv0560c* strains were plated on 7H11 agar with 4-, 5-, 10-, or 20-fold the IC_{90} of 14. Colonies visible after 3–5 wk were counted to measure frequency of resistance. These colonies were subjected to a second round of selection and then grown up in 7H9 medium with the corresponding concentration of 14 as a selection pressure. DNA was extracted using cetyltrimethylammonium bromide and lysozyme as described (42). The genomes of the resistant mutants characterized in this study were sequenced using an Illumina HiSeq 2500. The read length was between 54 bp and 125 bp (depending on sequencing run), and paired-end data were collected. Genome sequences were assembled by a comparative assembly method using custom-developed scripts for mapping reads and building contigs to identify indels, as described (43). Previously sequenced genomes of the parental strain (local stocks of Mtb H37Rv) for each of the mutants were used as reference sequences for the comparative assembly and for calling SNPs and other polymorphisms. Targeted sequencing (Macrogen Corp.) of *dpre1* and *rv2887* was performed after PCR amplification of the genes using the primers listed in *SI Appendix*, Table S2.

Transfer of SNPs Encoding Resistance to 14 into Wild-Type Mtb. Transfer of the SNPs encoding the R81Q and C-terminal deletion mutations in Rv2887 and the P116S, E221Q, G248S, and Y314H mutations in DprE1 into wild-type Mtb was performed by oligonucleotide-mediated recombineering as described (22),

using the oligonucleotides listed in *SI Appendix*, Table S2. Details of the method are included in *SI Appendix*.

RNASeq and qRT-PCR. Log-phase culture of Mtb H37Rv-North (Rv) and the clones resistant to 14, 1A and 8A, were treated with 3.9 μM of 14 or with vehicle control (1% DMSO) for 4 h. RNA was extracted and the mRNA was enriched using the MicrobExpress kit (Ambion). The cDNA libraries were synthesized according to instructions of the TruSeq RNA kit (LS protocol; Illumina), and RNA sequencing was performed with HiSeq2000/1000 (Illumina). The sequenced reads were aligned to the Mtb H37Rv complete genome (National Center for Biotechnology Information database) using Burrows–Wheeler alignment tool (44). The transcript abundances were measured in reads per kilobase of exon per million mapped reads (RPKM) using the Cufflinks package (45). Up- or down-regulated genes were identified based on the criteria that expression levels differed by >twofold relative to control and RPKM > 10 in all samples. Data are available at the GEO database (accession no. GSE77556). Reverse transcriptase (qScript cDNA synthesis kit from Quanta Biosciences)-generated cDNA was used for PCR amplification (PerfectA qPCR FastMix UNG from Quanta Biosciences) and quantification of *rv0560c*, *rv0559c*, *rv0558*, *rv0557*, and *rv2887* expression levels with *sigA* expression as the normalization control for cDNA input. Primer and probe sequences are listed in *SI Appendix*, Table S2.

EMSA Assay. Purified Rv2887 (wild type or R81Q) was incubated with 50 nM of a 70-mer spanning the promoter region of *rv0560c* (wild type or mutant; *SI Appendix*, Table S2) or 36-mer spanning *mbtB* promoter in binding buffer (pH 8) with 20 mM Tris·HCl, 50 mM KCl, 5 mM $MgCl_2$, 0.25 mg/mL BSA, and 10% glycerol for 10 min at room temperature. The samples were run in a 12% nondenaturing Tris-borate-EDTA (TBE) buffered gel for 1.75 h at 110V in 1× TBE buffer on ice. The gels were stained with a 1:10,000 dilution of SYBR Gold nucleic acid stain (Life Technologies) in 1× TBE buffer for 10 min at room temperature. Before loading the samples, the gel was prerun at 100 V for 30 min on ice. DNA bands were visualized with UV light using the Genius Bioimaging system (Syngene), and images were captured. ImageJ was used to quantify the intensity of the DNA bands (area under the peaks formed by bands). Values were normalized to control samples without Rv2887 protein and plotted against the protein/DNA ratio.

Methylation of 14 by Rv0560c. Initially, methylation of 14 by wild-type Rv0560c and S140A-Rv0560c was monitored using a coupled spectrophotometric assay as described (27). However, because of overlap in the absorption spectra of 14, the initial velocities could not be measured at 260 nm. Instead, the reaction was monitored at 380 nm due to the blue shift in the absorption spectra of 14 upon methylation. Upon confirmation of a dependence of the monitored initial velocity on the enzyme concentration, steady-state kinetic analysis of wild-type Rv0560c and S140A-Rv0560c was performed in a 96-well plate format using a SpectraMax M2 microplate reader. For SAM dependence, 25 μM 14, 25 nM MTAN, and 2 nM adenine deaminase were allowed to equilibrate at 37 °C in 10 mM phosphate buffer saline (2.7 mM KCl, 138 mM NaCl) with 10 mM $MgCl_2$, pH 7.4. The reaction was initiated by adding 670 nM wild-type enzyme or 600 nM S140A-Rv0560c. For substrate dependence, 96 μM SAM was used in the reaction mixture. The initial velocity was converted to units of concentration using an extinction coefficient (ε_{380nM}) of 13,200 $M^{-1}\cdot cm^{-1}$ for 14. The initial velocities were calculated and plotted using Prism. The kinetic parameters were also tested in the absence of the coupling enzymes using the same setup.

NMR-Based Determination of Methylation Site in 14. The methylation reaction was set up on a 15-mL scale with 25 μM 14, 96.5 μM SAM, 0.6 μM S140A-Rv0560c, 25 nM MTAN, and 2 nM adenine deaminase at 37 °C for about 15 h. The formation of the product was confirmed using LC-MS (363 *m/z* $[M+H]^+$). The methylated product was extracted using chloroform and purified using reverse phase column chromatography (XBridge prep C18, 5 μm) with a 5–95% gradient of acetonitrile/water with 0.1% TFA (flow rate 10 mL/min; retention time 12.2 min). The product was lyophilized and dissolved in 500 μL CDCl3 for identifying the site of methylation using NMR spectroscopy. All NMR spectra were acquired on a 600-MHz Brüker AVIII. A ^1H-^1H COSY (ns = 8) experiment was used to assign the ^1H spectra of 14 and 14-IA along with literature mining to confirm assignment of C-6 and C-9 protons of 14 and 14-IA. The gradient NOESY experiments for both 14 and 14-IA were performed with a mixing time of 0.8 s (ns = 32).

Quantification of Intrabacterial Amounts of 14 and me-14. H37Rv wild-type strain (Rv), Rv strain constitutively expressing *rv0560c*, resistant clones, 1A and 8A, H37Rv London Pride (LP), and Δ*rv0560c* strains were grown to log phase and inoculated on filters at a density of 3.5–5 × 10^8 bacteria per milliliter. The filters were transferred onto 7H10 agar plates and incubated at 37 °C for 5–7 d to allow bacterial growth. The filters were then exposed to 7.8 μM of 14 in 7H9 medium (without tyloxapol) for 24 h, and the metabolites were extracted with a mixture of acetonitrile:methanol:water (40:40:20) as described (46). The extracellular medium was also collected for analysis. LC-MS (46) was used to detect 14 (*m/z* of 349.16 in the positive mode) and me-14 (*m/z* of 363.18 in the positive mode) in the lysates and extracellular medium. BCA assay (Thermo Scientific) was used to measure protein amounts in the samples to normalize to sample biomass.

Enzyme Assay for DprE1. Compounds were dispensed in a black 384-well low-volume microplate (Greiner Bio-One) using a Hewlett Packard HP D300 digital dispenser (Tecan Group Ltd.). Preincubation mix (5 μL) containing 10 μM Rv0560c and 300 μM SAM in assay buffer (50 mM Hepes, pH 7.5, 100 mM NaCl, 100 μM Tween-20, 2 μM FAD, and 4 μM BSA) was added, and the reactions were incubated for 6.5 h at 25 °C to allow covalent modification of compounds. Substrate mix (5 μL) containing 1 mM FPR and 50 μM resazurin in assay buffer was then added (both are final assay concentrations). The DprE1 reactions were initiated immediately by adding enzyme mix (5 μL) containing 50 nM DprE1 in assay buffer and monitored spectrofluorimetrically using a Tecan Safire2 instrument (Tecan Group Ltd.). The DprE1 enzyme assay and data analysis have been described in detail (29).

ACKNOWLEDGMENTS. We are grateful to Tanya Parish at the Infectious Disease Research Institute for the Mtb strain deficient in *rv0560c* (Δ*rv0560c*) and its wild-type background strain, Mtb H37Rv London Pride (LP); and Stewart Cole at École Polytechnique Fédérale de Lausanne for Mtb strains carrying point mutations in DprE1. We thank James Sacchettini at Texas A&M University, Christopher Sassetti at University of Massachusetts Medical School, and Gurdyal Besra at University of Birmingham for guidance and support. We thank George Sukenick at the NMR facility at MSKCC and Jenny Xiang at the Genomics Core Facility at Weill Cornell Medicine for help with experimental setup and data collection. We are grateful for the help of Raquel Fernandez in synthesizing 14-IA and for the support of the TB unit in DDW-GlaxoSmithKline. Research performed in the M.L. laboratory was supported by NIGMS (2R01GM096056) and NIH/NCI Cancer Center Support Grant 5P30 CA008748-44. Work at Weill Cornell Medicine was supported by grants from the Bill & Melinda Gates Foundation (OPP1024029) and NIH (U19 AI111143-01, Tri-Institutional TB Research Unit). The Department of Microbiology & Immunology is supported by the William Randolph Hearst Trust.

1. World Health Organization (2014) *Global Tuberculosis Report 2014* (WHO Press, Geneva).
2. World Health Organization (2011) *Guidelines for the Programmatic Management of Drug-Resistant Tuberculosis: 2011 Update* (WHO Press, Geneva).
3. Pietersen E, et al. (2014) Long-term outcomes of patients with extensively drug-resistant tuberculosis in South Africa: A cohort study. *Lancet* 383(9924):1230–1239.
4. Nathan C (2012) Fresh approaches to anti-infective therapies. *Sci Transl Med* 4(140):140sr2.
5. Fox W, Ellard GA, Mitchison DA (1999) Studies on the treatment of tuberculosis undertaken by the British Medical Research Council tuberculosis units, 1946–1986, with relevant subsequent publications. *Int J Tuberc Lung Dis* 3(10, Suppl 2):S231–S279.
6. Johnson R, et al. (2006) Drug resistance in *Mycobacterium tuberculosis*. *Curr Issues Mol Biol* 8(2):97–111.
7. Nguyen L, Thompson CJ (2006) Foundations of antibiotic resistance in bacterial physiology: The mycobacterial paradigm. *Trends Microbiol* 14(7):304–312.
8. Aínsa JA, et al. (1998) Molecular cloning and characterization of Tap, a putative multidrug efflux pump present in *Mycobacterium fortuitum* and *Mycobacterium tuberculosis*. *J Bacteriol* 180(22):5836–5843.
9. Colangeli R, et al. (2005) The *Mycobacterium tuberculosis iniA* gene is essential for activity of an efflux pump that confers drug tolerance to both isoniazid and ethambutol. *Mol Microbiol* 55(6):1829–1840.
10. Flores AR, Parsons LM, Pavelka MS, Jr (2005) Genetic analysis of the beta-lactamases of *Mycobacterium tuberculosis* and *Mycobacterium smegmatis* and susceptibility to beta-lactam antibiotics. *Microbiology* 151(Pt 2):521–532.
11. Zaunbrecher MA, Sikes RD, Jr, Metchock B, Shinnick TM, Posey JE (2009) Overexpression of the chromosomally encoded aminoglycoside acetyltransferase eis confers kanamycin resistance in *Mycobacterium tuberculosis*. *Proc Natl Acad Sci USA* 106(47):20004–20009.
12. Buriánková K, et al. (2004) Molecular basis of intrinsic macrolide resistance in the *Mycobacterium tuberculosis* complex. *Antimicrob Agents Chemother* 48(1):143–150.
13. Warrier T, et al. (2015) Identification of novel anti-mycobacterial compounds by screening a pharmaceutical small-molecule library against non-replicating *Mycobacterium tuberculosis*. *ACS Infectious Diseases* 1(12):580–585.

14. Pethe K, et al. (2010) A chemical genetic screen in *Mycobacterium tuberculosis* identifies carbon-source-dependent growth inhibitors devoid of in vivo efficacy. *Nat Commun* 1:57.
15. Kelley LA, Mezulis S, Yates CM, Wass MN, Sternberg MJ (2015) The Phyre2 web portal for protein modeling, prediction and analysis. *Nat Protoc* 10(6):845–858.
16. Alekshun MN, Levy SB, Mealy TR, Seaton BA, Head JF (2001) The crystal structure of MarR, a regulator of multiple antibiotic resistance, at 2.3 Å resolution. *Nat Struct Biol* 8(8):710–714.
17. Alekshun MN, Kim YS, Levy SB (2000) Mutational analysis of MarR, the negative regulator of *marRAB* expression in *Escherichia coli*, suggests the presence of two regions required for DNA binding. *Mol Microbiol* 35(6):1394–1404.
18. Linde HJ, et al. (2000) In vivo increase in resistance to ciprofloxacin in *Escherichia coli* associated with deletion of the C-terminal part of MarR. *Antimicrob Agents Chemother* 44(7):1865–1868.
19. Duval V, McMurry LM, Foster K, Head JF, Levy SB (2013) Mutational analysis of the multiple-antibiotic resistance regulator MarR reveals a ligand binding pocket at the interface between the dimerization and DNA binding domains. *J Bacteriol* 195(15): 3341–3351.
20. George AM, Levy SB (1983) Amplifiable resistance to tetracycline, chloramphenicol, and other antibiotics in *Escherichia coli*: Involvement of a non-plasmid-determined efflux of tetracycline. *J Bacteriol* 155(2):531–540.
21. Ariza RR, Cohen SP, Bachhawat N, Levy SB, Demple B (1994) Repressor mutations in the *marRAB* operon that activate oxidative stress genes and multiple antibiotic resistance in *Escherichia coli*. *J Bacteriol* 176(1):143–148.
22. Murphy KC, Papavinasasundaram K, Sassetti CM (2015) Mycobacterial recombineering. *Methods Mol Biol* 1285:177–199.
23. Schuessler DL, Parish T (2012) The promoter of Rv0560c is induced by salicylate and structurally-related compounds in *Mycobacterium tuberculosis*. *PLoS One* 7(4):e34471.
24. Gold B, Rodriguez GM, Marras SA, Pentecost M, Smith I (2001) The *Mycobacterium tuberculosis* IdeR is a dual functional regulator that controls transcription of genes involved in iron acquisition, iron storage and survival in macrophages. *Mol Microbiol* 42(3):851–865.
25. Minch KJ, et al. (2015) The DNA-binding network of *Mycobacterium tuberculosis*. *Nat Commun* 6:5829.
26. Sassetti CM, Rubin EJ (2003) Genetic requirements for mycobacterial survival during infection. *Proc Natl Acad Sci USA* 100(22):12989–12994.
27. Dorgan KM, et al. (2006) An enzyme-coupled continuous spectrophotometric assay for *S*-adenosylmethionine-dependent methyltransferases. *Anal Biochem* 350(2):249–255.
28. Milano A, et al. (2009) Azole resistance in *Mycobacterium tuberculosis* is mediated by the MmpS5-MmpL5 efflux system. *Tuberculosis (Edinb)* 89(1):84–90.
29. Batt SM, et al. (2015) Whole cell target engagement identifies novel inhibitors of *Mycobacterium tuberculosis* decaprenylphosphoryl-b-D-ribose oxidase. *ACS Infectious Diseases* 1:615–626.
30. Makarov V, et al. (2009) Benzothiazinones kill *Mycobacterium tuberculosis* by blocking arabinan synthesis. *Science* 324(5928):801–804.
31. Wang F, et al. (2013) Identification of a small molecule with activity against drug-resistant and persistent tuberculosis. *Proc Natl Acad Sci USA* 110(27):E2510–E2517.
32. Neres J, et al. (2015) 2-Carboxyquinoxalines kill *mycobacterium tuberculosis* through noncovalent inhibition of DprE1. *ACS Chem Biol* 10(3):705–714.
33. Winglee K, Lun S, Pieroni M, Kozikowski A, Bishai W (2015) Mutation of Rv2887, a *marR*-like gene, confers *Mycobacterium tuberculosis* resistance to an imidazopyridine-based agent. *Antimicrob Agents Chemother* 59(11):6873–6881.
34. Alekshun MN, Levy SB (2007) Molecular mechanisms of antibacterial multidrug resistance. *Cell* 128(6):1037–1050.
35. Chakraborty S, Gruber T, Barry CE, 3rd, Boshoff HI, Rhee KY (2013) Para-aminosalicylic acid acts as an alternative substrate of folate metabolism in *Mycobacterium tuberculosis*. *Science* 339(6115):88–91.
36. Mathys V, et al. (2009) Molecular genetics of para-aminosalicylic acid resistance in clinical isolates and spontaneous mutants of *Mycobacterium tuberculosis*. *Antimicrob Agents Chemother* 53(5):2100–2109.
37. Brecik M, et al. (2015) DprE1 is a vulnerable tuberculosis drug target due to its cell wall localization. *ACS Chem Biol* 10(7):1631–1636.
38. Brugarolas P, et al. (2012) The oxidation-sensing regulator (MosR) is a new redox-dependent transcription factor in *Mycobacterium tuberculosis*. *J Biol Chem* 287(45): 37703–37712.
39. Healy C, Golby P, MacHugh DE, Gordon SV (2015) The MarR family transcription factor Rv1404 coordinates adaptation of Mycobacterium tuberculosis to acid stress via controlled expression of Rv1405c, a virulence-associated methyltransferase. *Tuberculosis (Edinb)* 97:154–162.
40. Ibáñez G, McBean JL, Astudillo YM, Luo M (2010) An enzyme-coupled ultrasensitive luminescence assay for protein methyltransferases. *Anal Biochem* 401(2):203–210.
41. Martin A, Camacho M, Portaels F, Palomino JC (2003) Resazurin microtiter assay plate testing of *Mycobacterium tuberculosis* susceptibilities to second-line drugs: Rapid, simple, and inexpensive method. *Antimicrob Agents Chemother* 47(11):3616–3619.
42. Larsen MH, Biermann K, Tandberg S, Hsu T, Jacobs WR (2007) Genetic manipulation of Mycobacterium tuberculosis. Current Protocols in Microbiology (Wiley, New York), Chap 10, Unit 10A.12.
43. Ioerger TR, et al. (2010) Variation among genome sequences of H37Rv strains of *Mycobacterium tuberculosis* from multiple laboratories. *J Bacteriol* 192(14):3645–3653.
44. Li H, Durbin R (2009) Fast and accurate short read alignment with Burrows–Wheeler transform. *Bioinformatics* 25(14):1754–1760.
45. Trapnell C, et al. (2013) Differential analysis of gene regulation at transcript resolution with RNA-seq. *Nat Biotechnol* 31(1):46–53.
46. Eoh H, Rhee KY (2013) Multifunctional essentiality of succinate metabolism in adaptation to hypoxia in *Mycobacterium tuberculosis*. *Proc Natl Acad Sci USA* 110(16): 6554–6559.